A WDM PAM4 FSO–UWOC Integrated System With a Channel Capacity of 100 Gb/s

Chung-Yi Li, Xu-Hong Huang, Hai-Han Lu, *Senior Member, IEEE, Senior Member, OSA*, Yong-Cheng Huang, Qi-Ping Huang, and Shi-Cheng Tu

***Abstract*—A wavelength-division-multiplexing (WDM) four-level pulse amplitude modulation (PAM4) free-space optical (FSO)–underwater wireless optical communication (UWOC) integrated system with a channel capacity of 100 Gb/s is proposed and attainably demonstrated. Analytic results reveal that 1.8-GHz 405-nm blue-violet-light and 1.7-GHz 450-nm blue-light laser diodes (LDs) with two-stage light injection and optoelectronic feedback techniques are competently adopted for 100 Gb/s PAM4 signal transmission through a 500-m free-space transmission with 5-m clear ocean underwater link. Combining dual-wavelength WDM scenario with PAM4 modulation, the channel capacity of FSO–UWOC integrated systems is significantly enhanced with an aggregate transmission rate of 100 Gb/s (25 Gbaud PAM4/wavelength × 2 wavelengths). With doublet lenses in FSO, laser beam reducer and transmissive spatial light modulator in UWOC, a sufficiently low bit error rate of 10^{-9} and acceptable PAM4 eye diagrams are acquired. This demonstrated 100 Gb/s PAM4 FSO–UWOC integrated system with a WDM scenario is advantageous for the enhancement of a high-speed optical wireless link with long-reach transmission.**

***Index Terms*—Four-level pulse amplitude modulation (PAM4), free-space optical (FSO), underwater wireless optical communication (UWOC), wavelength-division-multiplexing (WDM).**

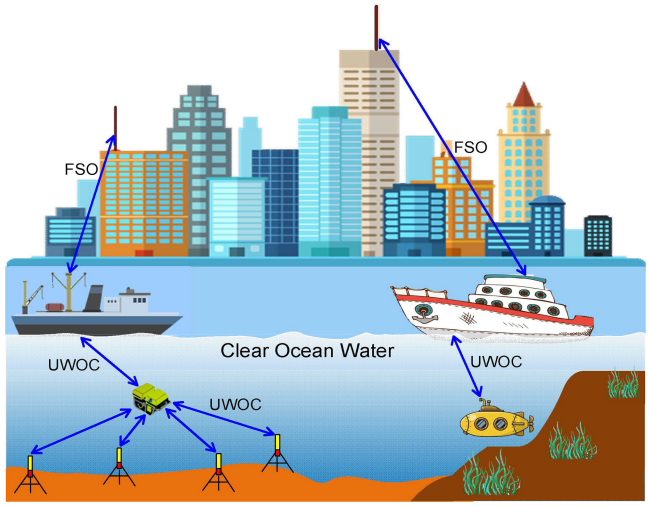

Fig. 1. A high-speed FSO–UWOC integrated system with long-range transmission. FSO, free-space optical; UWOC, underwater wireless optical communication.

I. Introduction

FREE-SPACE optical (FSO) communication is an optical communication technology that utilizes light transmitting in free-space to transport data wirelessly for high-speed Internet, wireless broadband access, and mobile telecommunication [1], [2]. Underwater wireless optical communication (UWOC) systems present a platform for supporting present and developing applications, such as sea-floor resource mining, offshore exploration, and real-time high-definition video transmissions over UWOC [3], [4]. FSO–UWOC integrated systems are thereby developed to supply high-speed and long-range optical wireless transmissions utilizing an optical beam with huge bandwidth. Owing to the fast evolution of FSO–UWOC integrated systems, they can deliver some tens gigabit data rate over a free-space link with an underwater channel [5]–[7]. With the rising demands for FSO–UWOC integration, constructing a high-speed FSO–UWOC integrated system with long-range transmission (as illustrated Fig. 1) is critically important. In this study, a 100-Gb/s dual-wavelength wavelength-division-multiplexing (WDM) four-level pulse amplitude modulation (PAM4) FSO–UWOC integrated system utilizing 405-nm blue-violet-light and 450-nm blue-light laser diodes (LDs) with two-stage light injection and optoelectronic feedback techniques through 500 m free-space transmission and 5 m clear ocean underwater link is attainably built. By making good use of clear ocean water's low absorption in blue-violet-light and blue-light wavelengths (400–450 nm) [8], [9], 405-nm blue-violet-light and 450-nm blue-light LDs are utilized in this constructed FSO–UWOC integrated system. Additionally, LD with two-stage light injection and optoelectronic feedback techniques achieves a considerable 3-dB bandwidth and optical output power enhancements [10]. The aggregate channel capacity is remarkably improved by simultaneously adopting dual-wavelength WDM scenario and

Manuscript received August 27, 2019; revised November 1, 2019 and December 8, 2019; accepted December 15, 2019. Date of publication December 18, 2019; date of current version April 1, 2020. This work was supported by Qualcomm through Taiwan University Research Collaboration Project under Grant NTA-414684. *(Corresponding author: Hai-Han Lu.)*

C.-Y. Li is with the Department of Communication Engineering, National Taipei University, New Taipei City 23741, Taiwan (e-mail: cyli@mail.ntpu.edu.tw).

X.-H. Huang is with the School of Information Science and Engineering, Fujian University of Technology, Fuzhou 350118, China (e-mail: huangxuh1@163.com).

H.-H. Lu, Y.-C. Huang, Q.-P. Huang, and S.-C. Tu are with the Institute of Electro-Optical Engineering, National Taipei University of Technology, Taipei 10608, Taiwan (e-mail: hhlu@ntut.edu.tw; bighead70137@gmail.com; whanh1099@gmail.com; tu90004906@yahoo.com.tw).

Color versions of one or more of the figures in this article are available online at http://ieeexplore.ieee.org.

Digital Object Identifier 10.1109/JLT.2019.2960525

PAM4 modulation in an FSO–UWOC integrated system. WDM scenario, which employs different wavelengths to deliver the combined optical signals, is expected to afford high channel capacity in FSO communications [11], [12]. PAM4's bandwidth is half of non-return-to-zero (NRZ), causing PAM4 modulation promising in high-transmission-rate communications [13]–[15]. Combining the WDM scenario and PAM4 format, the aggregate transmission rate of the dual-wavelength WDM PAM4 FSO–UWOC integrated system is substantially enhanced four times [2 (dual-wavelength WDM scenario) $\times$ 2 (PAM4 modulation) $=$ 4]. We practically demonstrate an FSO–UWOC integrated system with a gross transmission rate of 100 Gb/s (50 Gb/s PAM4/wavelength $\times$ 2 wavelengths). With doublet lenses in FSO communications, laser beam reducer and spatial light modulator (SLM) in UWOC systems [16], [17], a sufficiently low bit error rate (BER) of 10^{-9} and acceptable PAM4 eye diagrams are attained through 500 m free-space transmission and 5 m clear ocean underwater link. A couple of doublet lenses play vital roles for transmitting a laser beam through 500 m free-space transmission. Utilizing a laser beam reducer to decrease beam size, the UWOC system's transmission quality can be enhanced on account of less light absorbed by clear ocean water [9], [17]–[19]. One of the major challenges in UWOC systems is the flow of ocean. In a practical scenario, a laser beam misalignment owing to flow of ocean will cause link unreliability and performance degradation [20], [21]. A transmissive SLM with an electrical controller is thereby operated as a flexible convex lens [22] to implement beam size reduction and mitigate laser beam misalignment because of oceanic turbulence induced by flow of ocean.

Our previous study demonstrated a 256-Gb/s four-channel space-division-multiplexing (SDM)-based PAM4 FSO–UWOC integrated system [5]. The 50 m free-space transmission in our previous work is much shorter than the associated value of 500 m operated in this proposal. Moreover, four couples of doublet lenses are required to establish such complicated four-channel SDM FSO–UWOC integrated system. For a real realization of an FSO–UWOC integrated system, it is essential to construct a framework with the advantage of low complexity. In addition, SDM-based PAM4 FSO–UWOC integration has large room for improvement when one considers the stringent optical alignment requirement in practical scenarios. UWOC systems cannot provide stable air-water-air interface transmission due to severe beam alignment request. This can pose a serious challenge, particularly in the presence of oceanic turbulence that produces misalignment because of ocean flow. This newly proposed WDM-based PAM4 FSO–UWOC integrated system resolves the difficult problem that oceanic engineering is currently working on resolving. In comparison with an SDM-based FSO–UWOC integrated system, this proposed WDM-based FSO–UWOC integrated system is notable for its simplicity and practicality. Sun *et al*. achieved a diffuse-line-of-sight communication across a wavy water-air interface based on NRZ on-off keying (OOK) and quadrature amplitude modulation (QAM)-orthogonal frequency-division multiplexing (OFDM) modulations [23]. However, the modulation can be enhanced and simplified by adopting PAM4 modulation. Compared with NRZ-OOK, PAM4 provides 2 bits for each symbol with high channel capacity and low bandwidth advantages. In terms of QAM, the QAM receiver is more complicated compared to a receiver with another modulation format. Regarding OFDM, its chief problem is its high peak-to-average power ratio (PAPR). It is critically important to deal with PAPR reduction in OFDM systems to avoid performance degradation. Compared with QAM-OFDM (with a power dissipation of 4135 mW), PAM4 (with a power dissipation of 1235 mW) is better owing to its system simplicity and low power trait [24]. Additionally, given that the transmission rate will be greatly reduced with the utilization of diffuse-line-of-sight scheme, the 11.4 Mb/s (8-QAM-OFDM) and 55 Mb/s (NRZ-OOK) transmission rates are significantly less than that of the 100 Gb/s delivered in this proposed integrated system. Zhang *et al*. demonstrated a two-path parallel scheme for m-QAM-OFDM transmission through a turbulent-air-water channel in optical wireless communications [25]. An atmospheric turbulence simulator is adopted to provide a 7.5-m turbulent air channel. Results show that the generated turbulence is weak for the air channel when the temperature reaches 50 °C. The 8-m underwater channel is somewhat longer than the related length of 5 m implemented in the demonstrated integrated system. Nevertheless, the 7.5-m air channel and the 668.34 Mb/s (16-QAM-OFDM)/1 Gb/s (64-QAM-OFDM) data rate are notably lower than the associated 500 m and 100 Gb/s adopted in this proposal. Zhao *et al*. developed a feedback-enabled adaptive underwater twisted light transmission link utilizing the reflection at the air-water interface [26]. However, a complicated adaptive feedback system is needed to provide a stable output. Moreover, the 2-m underwater link is considerably shorter than the total link of 505 m implemented in our proposed system. Wang *et al*. showed favorable performance of the feedback-assisted water-air-water twisted light data information transfer with orbital angular momentum (OAM) [27]. Nonetheless, the 1.08-Gbit/s data rate is considerably lower than the 100-Gb/s total data rate utilized in this proposed FSO–UWOC integration. Chen *et al*. presented a 5.5 Gb/s data rate through a 5-m air link and 21-m underwater channel with OFDM modulation [28]. Although the 21-m underwater channel of is longer than the 5-m implemented in the demonstrated integrated system, the 5-m air link and the 5.5-Gb/s data rate are notably lower than the 500-m and 100-Gb/s adopted in this proposal. Furthermore, the performance of underwater channel with oceanic turbulence due to ocean flow has not been verified.

With the adoption of dual-wavelength WDM scenario and PAM4 modulation, a 100-Gb/s FSO–UWOC integrated system is attainably constructed. The contributions of this study can be summarized as follows:

(I) A long-reach 500-m free-space transmission and 5-m clear ocean underwater link is attained.

(II) Significant improvements in 3-dB bandwidth and optical output power are acquired utilizing 405/450 nm blue-violet-light/blue-light LDs with two-stage light injection and optoelectronic feedback techniques.

(III) Integrating the WDM scenario with PAM4 modulation, the channel capacity is considerably enhanced by four times with a gross transmission rate of 100 Gb/s.

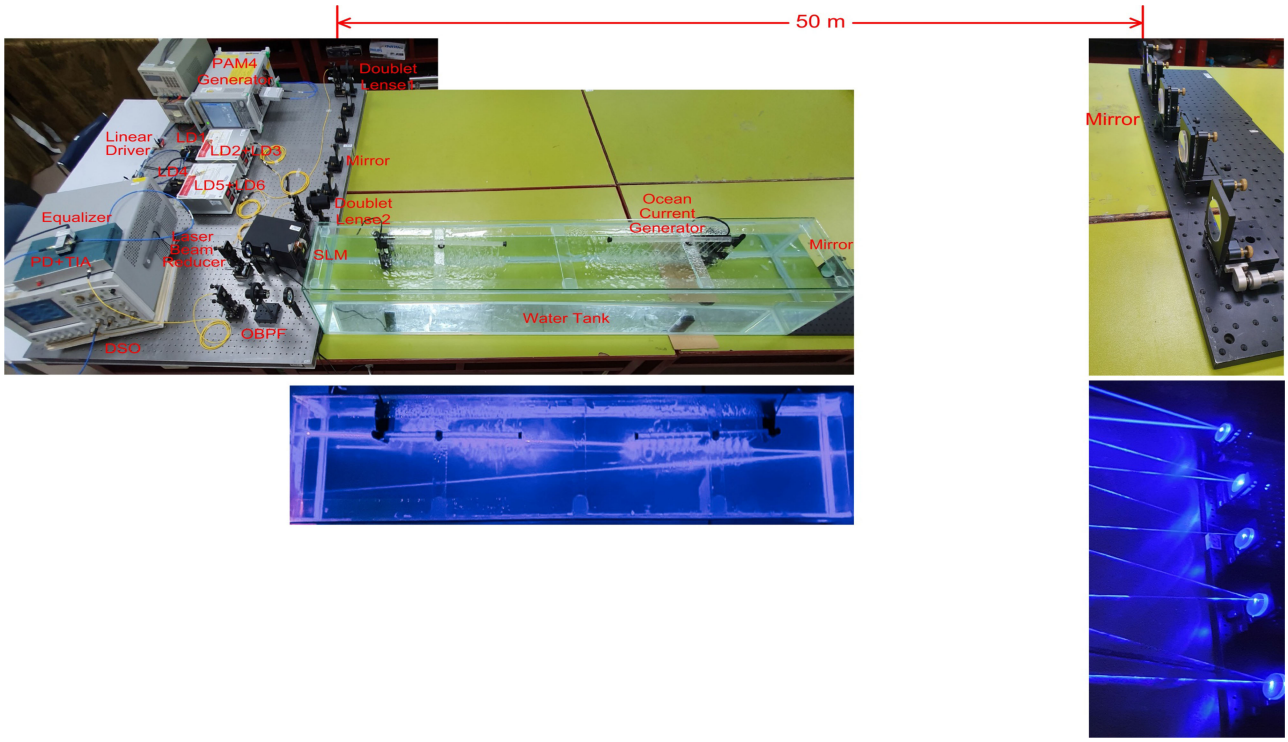

Fig. 2. The photo of the demonstrated experimentation using a laboratory setup.

(IV) Employing a set of doublet lenses in FSO communications, a laser beam reducer and a transmissive SLM in UWOC links, an impressively low BER of 10^{-9} and acceptable PAM4 eye diagrams are obtained.

This demonstrated 100 Gb/s dual-wavelength WDM-based PAM4 FSO–UWOC integrated system enables a useful selection for high aggregate channel capacity and develops the state realized by the integration of FSO communications with UWOC links. This system is better than existing FSO–UWOC integrations given it offers a high-transmission optical wireless link with long-range transmission.

II. Experimental Setup

Fig. 2 presents the photo of the demonstrated experimentation using a laboratory setup. And further, Fig. 3 presents the structure of the demonstrated 100 Gb/s dual-wavelength WDM-based PAM4 FSO–UWOC integrated system using blue-violet-light/blue-light LDs with two-stage light injection and optoelectronic feedback techniques through 500 m free-space transmission and 5 m clear ocean underwater link. A 50 Gb/s PAM4 signal generated from a PAM4 signal generator (Anritsu MP1800A), with a pseudorandom binary sequence length of 2^{15}-1, is split by a 1×2 power divider. After being electrically driven by a linear driver (Tektronix PSPL5882), the 50 Gb/s PAM4 signal is supplied in LD1/LD4 (Thorlabs LP405-SF30/LP450-SF15), with central wavelength of 405.01 nm/450 nm and 3-dB bandwidth of 1.8 GHz/1.7 GHz. LD1's/LD4's output is injected into LD2/LD5 (404.88 nm/449.87 nm) via first-stage light injection and optoelectronic feedback techniques. Subsequently, the output of injection-locked LD2/LD5 (405.01 nm/450 nm) is injected into LD3/LD6 (405.13 nm/450.12 nm) via second-stage light injection and optoelectronic feedback techniques. An optical isolator is deployed in each stage to keep the laser light emitted from the LD with light injection and optoelectronic feedback. Several devices, including three LDs (LD1, LD2, and LD3; LD4, LD5, and LD6), two optical isolators, four optical couplers, two polarization controllers, and two photodiode (PD) with trans-impedance amplifier (TIA) receivers, are used for two-stage light injection and optoelectronic feedback schemes. However, these devices are worth using because an LD with two-stage light injection and optoelectronic feedback techniques attains significant 3-dB bandwidth and optical output power improvements.

The laser lights sent out from the LDs with two-stage light injection and optoelectronic feedback techniques are integrated by a 2×1 optical combiner with a gross transmission rate of 100 Gb/s (50 Gb/s/wavelength $\times$ 2 wavelengths), and supplied in a 500-m free-space link using a set of doublet lenses. Through 500 m free-space link, the laser beam is transmitted to a laser beam reducer so as to enhance underwater transmission qualities. A transmissive SLM (Meadowlark MSP1920), with a short response time of 5 ms and a high transmittance of 95%, functions as a convex lens to perform laser beam reduction. In addition, an electrical controller is utilized to control the SLM, enabling it to adaptively alleviate the turbulence induced by the flow of ocean. The reduced laser beam is transmitted across a rectangular water tank with 2.5 m (length) $\times$ 0.5 m (width) $\times$ 0.5 m (height) dimensions. The rectangular water tank is filled with clear ocean water with a particle concentration of 3.86 g/m^3.

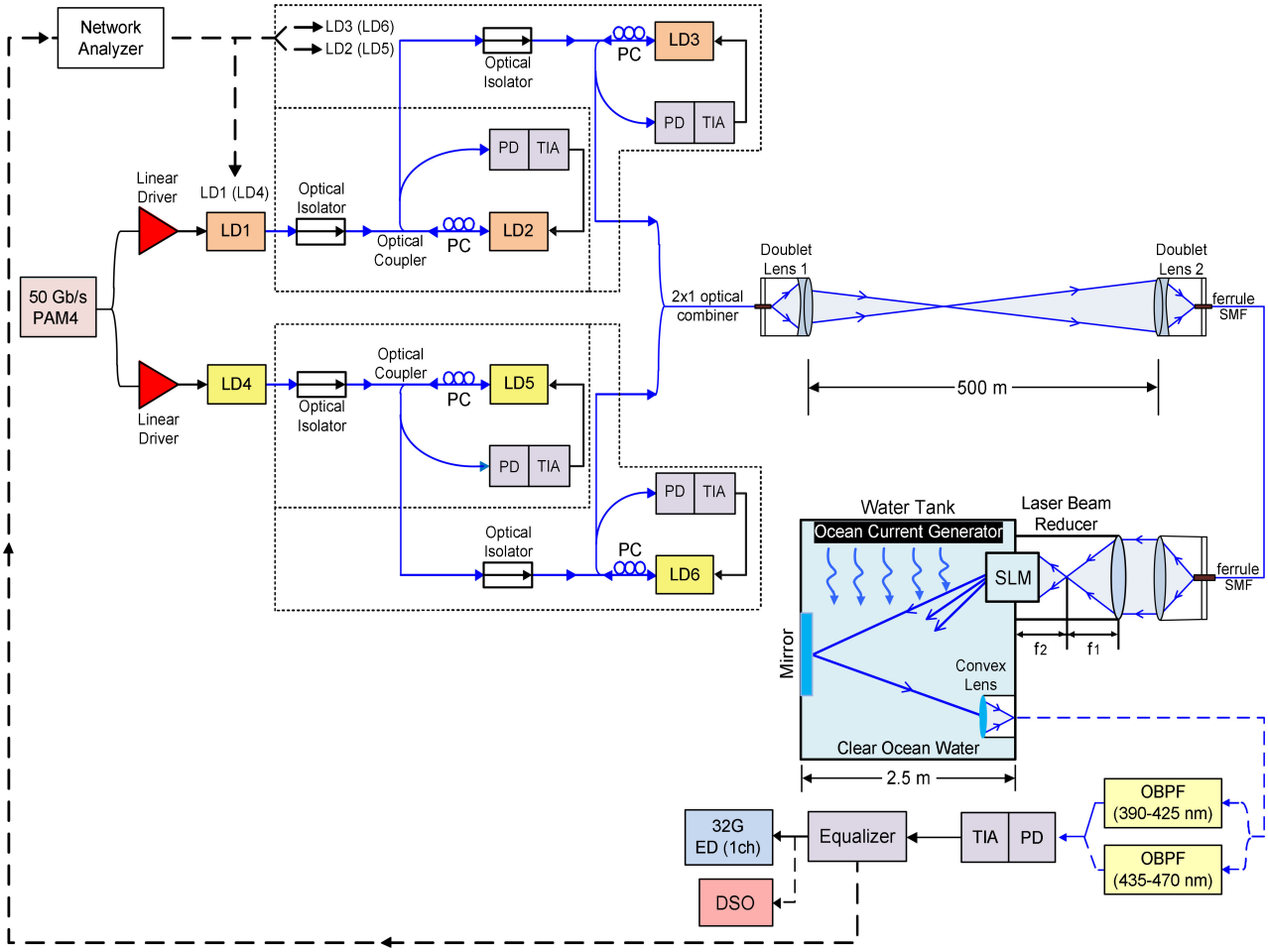

Fig. 3. Structure of the demonstrated 100 Gb/s dual-wavelength WDM-based PAM4 FSO–UWOC integrated system through 500 m free-space transmission and 5 m clear ocean underwater link. WDM: wavelength-division-multiplexing; PAM4: four-level pulse amplitude modulation; LD: laser diode; PD: photodiode; TIA: trans-impedance amplifier; SLM: spatial light modulator; OBPF: optical band-pass filter; ED: error detector; DSO: digital storage oscilloscope.

The particle concentration of clear ocean water is produced with suspensions of $Al(OH)_3$ and $Mg(OH)_2$, which is acquired by inserting a commercial antacid preparation (Maalox) [29], [30]. It is usually utilized in a laboratory experiment for providing the required particle concentration. Given that the average speed of the ocean current is 1.5 m/sec [31], an ocean current generator with a speed of 1.5 m/sec is deployed to simulate the flow of ocean. The reduced and controlled laser beam is transported in a clear ocean underwater channel. A reflective mirror reflects the laser beam, and a convex lens concentrates it. The laser beam travels through an optical band-pass filter, with a passband window of 390–425 nm (Techspec Filters OD5)/435–470 nm (Techspec Filters OD6), to choose the desired wavelength. The chosen wavelength (laser beam) is received and enhanced by a 23-GHz PD with a TIA (Optilab PR-23-M) receiver. The enhanced 50 Gb/s PAM4 signal is inputted into an equalizer (Anritsu AH54147A) for signal equalization. After equalization, a real-time BER measurement is implemented utilizing a high-sensitivity error detector (ED) (Anritsu MP1800A 28 Gb/s ED) and the PAM4 three-eye sampling way. It is attractive because it avoids the requirement of complex off-line digital signal processing using Matlab. In addition, a digital storage oscilloscope (Keysight N1000A DCA-X) is adopted to catch the eye diagrams of transmitted 50 Gb/s PAM4 signal.

Fig. 3 shows the frequency response measurement setup of dual-wavelength WDM PAM4 FSO–UWOC integration as well. A sweep signal (DC – 20 GHz) produced from a network analyzer (Anritsu MS4644A) sends to the blue-violet-light/blue-light LDs. After electrical equalization by an equalizer, the sweep signal returns to the network analyzer. Eventually, the frequency response of the dual-wavelength WDM PAM4 FSO–UWOC integrated system is measured in the free-running (LD1/LD4), one-stage light injection and optoelectronic feedback (injection-locked LD2/LD5), and two-stage light injection and optoelectronic feedback (injection-locked LD3/LD6) states.

A set of doublet lenses, as illustrated in Fig. 4, are adopted to send the laser beam to a free-space and to conduct the beam to the fiber's ferrule. The free-space transmission distance is extended to 500 m (50 m $\times$ 10), with the deployment of reflective mirrors on both sides. At the receiving end, a convergent setup should be deployed to couple the laser beam with the fiber's ferrule. The operation of doublet lens 2 is to couple the laser beam with the fiber's ferrule. A doublet lens (AC508-150-C), with focal length/back focal length/diameter of 150 mm/150 mm/

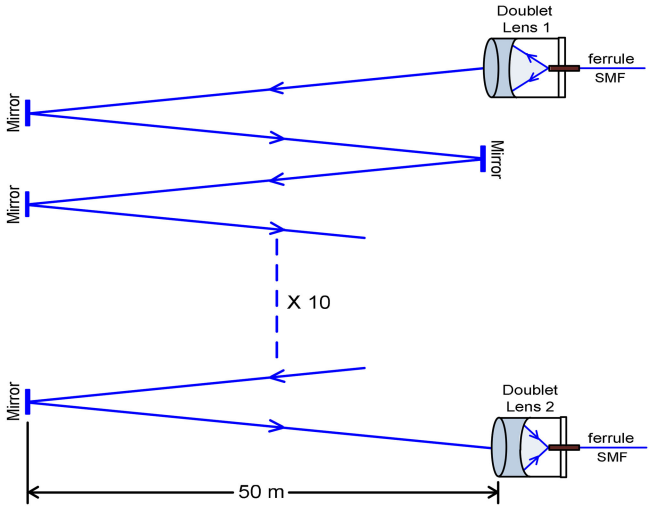

Fig. 4. A set of doublet lenses send the laser beam to a free-space and conduct the beam to the fiber's ferrule.

50.8 mm, comprises two lenses (concave and convex) that are paired together. The single-mode fiber's numerical aperture is 0.14; therefore, the laser beam's diameter (d) can be calculated as:

$$d = 2 \times (150 \times 0.14) = 42 \ \text{(mm)} \tag{1}$$

Since doublet lens 1's diameter (50.8 mm) is larger than the laser beam's diameter (42 mm), a free-space transmission with doublet lens 1 is feasible. Over an L-m free-space link, the laser beam's diameter (d_L) must be lesser than that of doublet lens 2 ($d_L < 50.8$ mm) to make a free-space transmission with doublet lens 2 feasible:

$$d_L = \sqrt{d^2 + (2\theta L)^2} = \sqrt{42^2 + (0.048L)^2} < 50.8 \tag{2}$$

where θ is the beam divergence. L is computed as 595.4, indicating that the maximum free-space link is 595.4 m. The free-space link adopted in this work is 500 m (<595.4 m) to satisfy the maximum free-space link target. A set of fiber collimators with convex lenses might be adopted to substitute for a set of doublet lenses and establish a 500-m free-space link. Nonetheless, it is a challenge to establish a 500-m free-space link utilizing a set of fiber collimators with convex lenses. The collimated laser beam emitted from a fiber collimator with a convex lens will spread as it travels through a certain free-space distance. In a free-space link of 500 m, the laser beam's diameter will be larger than that of doublet lens 2 (>50.8 mm). With a large beam diameter, the convex lens with a fiber collimator will accumulate less transmitted light. An obvious decrease in the received optical power occurs, which is followed by poor BER performance.

III. Experimental Results and Discussions

FSO communications are influenced by atmospheric turbulence, which will produce atmospheric attenuation as the optical signal passes through the free-space link. For FSO communications, the atmospheric attenuation coefficient changes with different weather types. Atmospheric attenuation is determined by the atmospheric particle size in relation to the optical wavelength. In clear weather, the atmospheric particle size is comparatively small, whereas it is comparatively large in bad weather. Through 500 m free-space transmission, the atmospheric attenuation varies from 1.2 dB (good weather) to 50 dB (bad weather) [32]. The performance of FSO communications is susceptible to bad weather, it deteriorates during heavy fog, heavy snow, and heavy rain scenarios. Serious atmospheric turbulence due to bad weather will severely influence the link availability of FSO communications and lead to poor BER [33]. During heavy fog, heavy snow, and heavy rain scenarios, however, the millimeter-wave (MMW) connection can be employed as an alternate solution [34]. In this work, an atmospheric attenuation of around 1.5 dB occurs owing to 500 m free-space transmission, and an atmospheric link loss of about 0.8 dB occurs because of noise from environmental lights. The actual loss of the atmospheric link is increased as other lights from the environment are received. Thus, an actual loss of the atmospheric link of 2.3 dB (1.5 + 0.8) exists, which is considerably less than the worst case of 50 dB/500 m. Conclusively, a 500-m free space transmission with a set of doublet lenses meets the target of high link availability.

In an underwater channel, the overall underwater losses can be expressed by the attenuation coefficient $c(\lambda)$ ($= a(\lambda) + b(\lambda)$) at a certain wavelength λ. $a(\lambda)$ and $b(\lambda)$ are the absorption and the scattering coefficients, respectively. These coefficients change with different water types and optical wavelengths [35]–[38]. In a clear ocean underwater channel, the coefficients of $a(\lambda)$, $b(\lambda)$ and $c(\lambda)$ in blue-violet-light/blue-light wavelengths (400–450 nm) are 0.114, 0.037, and 0.151 (m^{-1}), respectively [39]–[41]. The absorption coefficient $a(\lambda)$ offers 3.1 times the value of scattering coefficient $b(\lambda)$ (0.114/0.037 $\sim$ 3.1), signifying that absorption is the main contributor in a clear ocean underwater link. Due to the product conservation of beam size and beam divergence, a laser beam reducer for beam size reduction will expand the beam divergence. For a clear ocean underwater channel, given that the ratio of the scattered light is small, a small beam size that follows a large beam divergence will not produce large performance degradation. Moreover, optical misalignment in UWOC systems will severely affect its link and reliability. A transmissive SLM with short response time is thereby adopted to mitigate these problems, which not only allows the laser beam to be adaptively transmitted to develop a practical FSO–UWOC integration, but also conquers oceanic engineering problems to construct a reliable UWOC link [42]. Given that the average speed of an ocean current is $\sim$1.5 m/sec, the response time of a transmissive SLM ($\sim$5 ms) can certainly meet the target for adjusting the laser beam in UWOC systems. Oceanic turbulence induced by flow of ocean becomes strong enough to influence the UWOC link when strong ocean current (>2.5 m/sec) occurs. Because the transmissive SLM response time is not short enough, oceanic turbulence due to strong ocean current will strictly affect the UWOC link and result in worse BER performance.

The optical transmittance with particle concentrations of 0.3 (piped water), 3.86 (clear ocean water), 23.54, and 30.24 g/m^3 (turbid water) are presented in Fig. 5. It is to be found that as the particle concentration increases, the optical transmittance

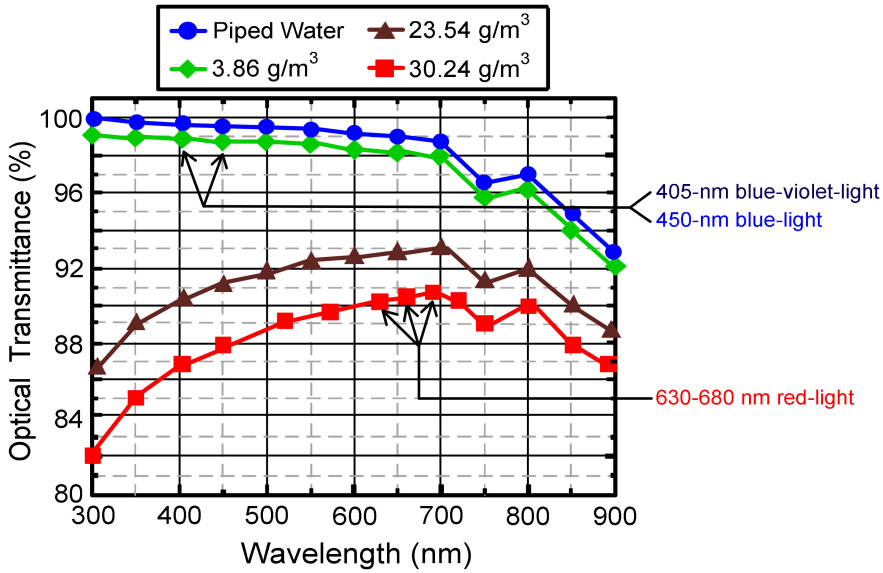

Fig. 5. The optical transmittances with different particle concentrations: 0.3 (piped water), 3.86 (clear ocean water), 23.54, and 30.24 g/m^3 (turbid water).

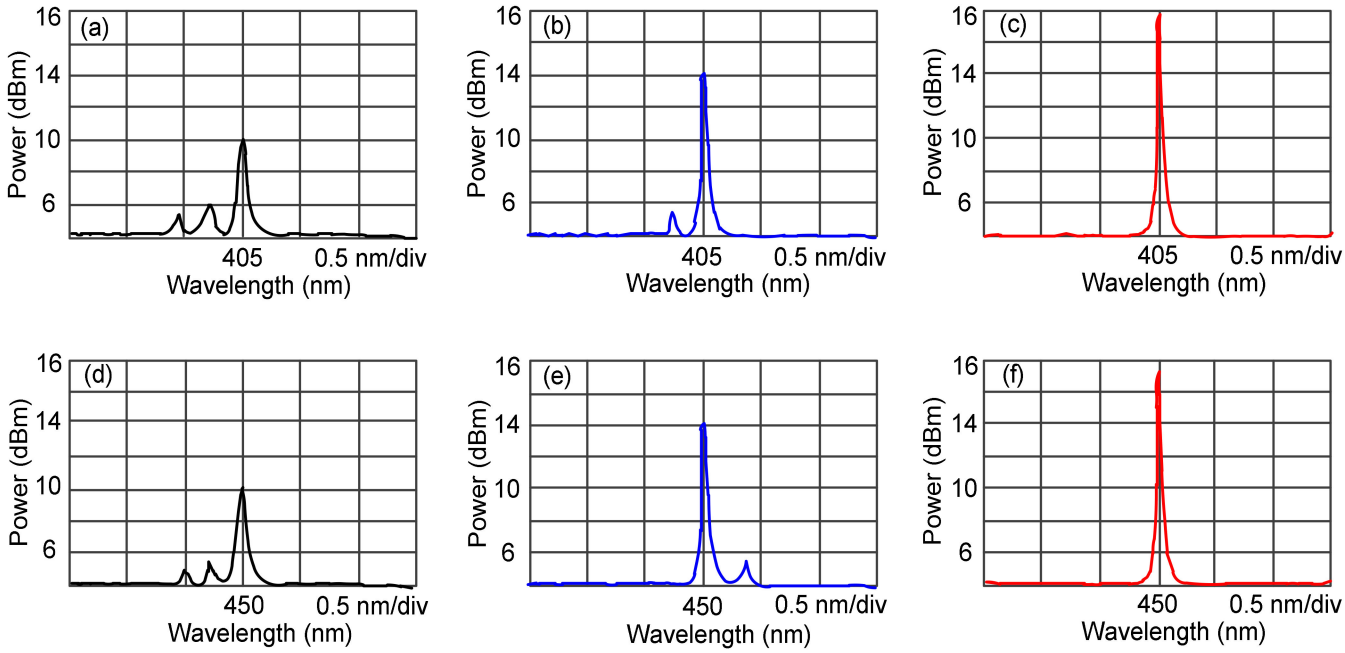

Fig. 6. Optical spectra of (a) LD1 in free-running state, (b) LD2 with light injection and optoelectronic feedback techniques locked at 405.01 nm, (c) LD3 with light injection and optoelectronic feedback techniques locked at 405.01 nm, (d) LD4 in free-running state, (e) LD5 with light injection and optoelectronic feedback techniques locked at 450 nm, and (f) LD6 with light injection and optoelectronic feedback techniques locked at 450 nm.

decreases [43]. With 3.86 g/m^3 particle concentration (clear ocean water), the optical transmittance in 405 nm/450 nm blue-violet-light/blue-light wavelength is higher than that in 630–680 nm red-light wavelength. With 30.24 g/m^3 particle concentration (turbid water), however, the optical transmittance in the 405 nm/450 nm blue-violet-light/blue-light wavelength is lower than that in 630–680 nm red-light wavelength. Results reveal that 405 nm blue-violet-light and 450 nm blue-light LDs are appropriate for a clear ocean underwater channel, whereas 630–680 nm red-light laser is appropriate for a turbid underwater channel [44], [45].

Fig. 6(a)/Fig. 6(d) shows the LD1/LD4 optical spectrum in free-running state. Fig. 6(b)/Fig. 6(e) exhibits the LD2/LD5 optical spectrum with light injection and optoelectronic feedback techniques locked at 405.01 nm/450 nm. The injection-locked LD2/LD5 optical spectrum moves to a relatively longer

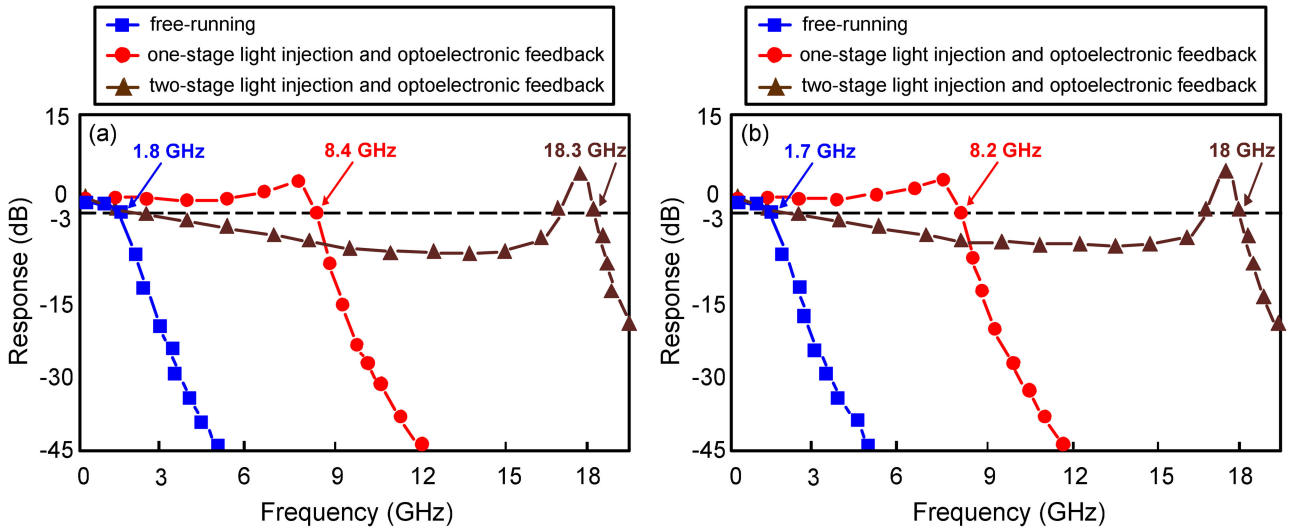

Fig. 7. (a) The 3-dB bandwidths for the free-running (LD1), one-stage light injection and optoelectronic feedback (injection-locked LD2), and two-stage light injection and optoelectronic feedback (injection-locked LD3) scenarios. (b) The 3-dB bandwidths for the free-running (LD4), one-stage light injection and optoelectronic feedback (injection-locked LD5), and two-stage light injection and optoelectronic feedback (injection-locked LD6) scenarios.

wavelength (404.88 nm/449.87 nm $\rightarrow$ 405.01 nm/450 nm). First-stage light injection and optoelectronic feedback behaviors happen as a master laser (LD1/LD4) is slightly adjusted to a wavelength that is longer than that of the slave laser (LD2/LD5). Moreover, it is to be observed that the peak powers of injection-locked LDs (LD2 and LD5) are obviously increased. Fig. 6(c)/Fig. 6(f) presents the LD3/LD6 optical spectrum with light injection and optoelectronic feedback techniques locked at 405.01 nm/450 nm. The injection-locked LD3/LD6 optical spectrum moves to a relatively shorter wavelength (405.13 nm/450.12 nm $\rightarrow$ 405.01 nm/450 nm). Second-stage light injection and optoelectronic feedback behaviors happen as a master laser (LD2/LD5) is slightly detuned to a wavelength that is shorter than that of the slave laser (LD3/LD6). Furthermore, it is to be found that the peak powers of injection-locked LDs (LD3 and LD6) are remarkably increased.

In addition, it should be noted that an LD with two-stage light injection and optoelectronic feedback techniques attains a considerable 3-dB bandwidth improvement. 3-dB bandwidth is an important figure-of-merit that describes the quality of an LD. Figs. 7(a) and 7(b) exhibit the 3-dB bandwidths for the free-running (LD1/LD4), one-stage light injection and optoelectronic feedback (injection-locked LD2/LD5), and two-stage light injection and optoelectronic feedback (injection-locked LD3/LD6) scenarios. Clearly, the operating bandwidth reaches up to 18.3 GHz/18 GHz (1.8 GHz/1.7 GHz $\rightarrow$ 18.3 GHz/18 GHz). Two-stage light injection and optoelectronic feedback is recognized as one of the most favorable solutions to overcome the bandwidth limitation. The operating bandwidth can be extensively increased using two-stage light injection and optoelectronic feedback techniques. Furthermore, the modulation response is performed by descent in the middle frequencies and a resonance peak in the high frequencies to attain a great 3-dB bandwidth improvement. Because the 18.3 GHz/18 GHz is located at the resonance peak, the drop in the middle frequencies will not influence the transmission performance. Provided that the transmission rate is $\sqrt{2}$ times the bandwidth [18], the maximum channel capacity can reach 101.82 Gb/s [$18 \times \sqrt{2} \times 2$ (dual-wavelength WDM scenario) $\times$ 2 (PAM4 modulation) $=$ 101.82] by adopting dual-wavelength WDM scenario and PAM4 modulation.

Fig. 8(a) presents the BER performances of the 50 Gb/s PAM4 signal at a chosen wavelength of 405.01 nm in the states of back-to-back (BTB), through 500 m free-space transmission (500-m FSO), and through 500 m free-space transmission with 5 m clear ocean underwater link (505-m FSO–UWOC). Moreover, Fig. 8(b) presents the BER values of the 50 Gb/s PAM4 signal at a chosen wavelength of 450 nm in different scenarios. BTB means that the transmitting side and the receiving end are directly connected, and there is no need to transmit an optical signal through the free-space transmission with an underwater link. These two figures show that the BER curves at the chosen wavelengths of 405.01 and 450 nm are almost similar, revealing that the influences for transmission performance at these selected wavelengths are nearly the same. At a BER value of 10^{-9}, a 3.2-dB [Fig. 8(a)]/3.4-dB [Fig. 8(b)] power penalty emerges between the BTB state and that through a 500-m free-space transmission. The 3.2 dB/3.4 dB power penalty chiefly results from the atmospheric attenuation on account of 500 m free-space transmission, atmospheric link loss owing to the noise from environmental lights, and coupling loss from the laser beam coupling to the fiber's ferrule. A 500-m free-space transmission causes somewhat atmospheric attenuation and brings on a reduced BER performance. Moreover, noise is produced when other lights from the environment are received. Furthermore, laser beam alignment is critically important to the performance of FSO communications. It is imperative for a laser beam to match the fiber collimator's field of view (FOV) to sustain the link availability of FSO communications. Laser beam mismatch that accompanies a large coupling loss will bring on worse

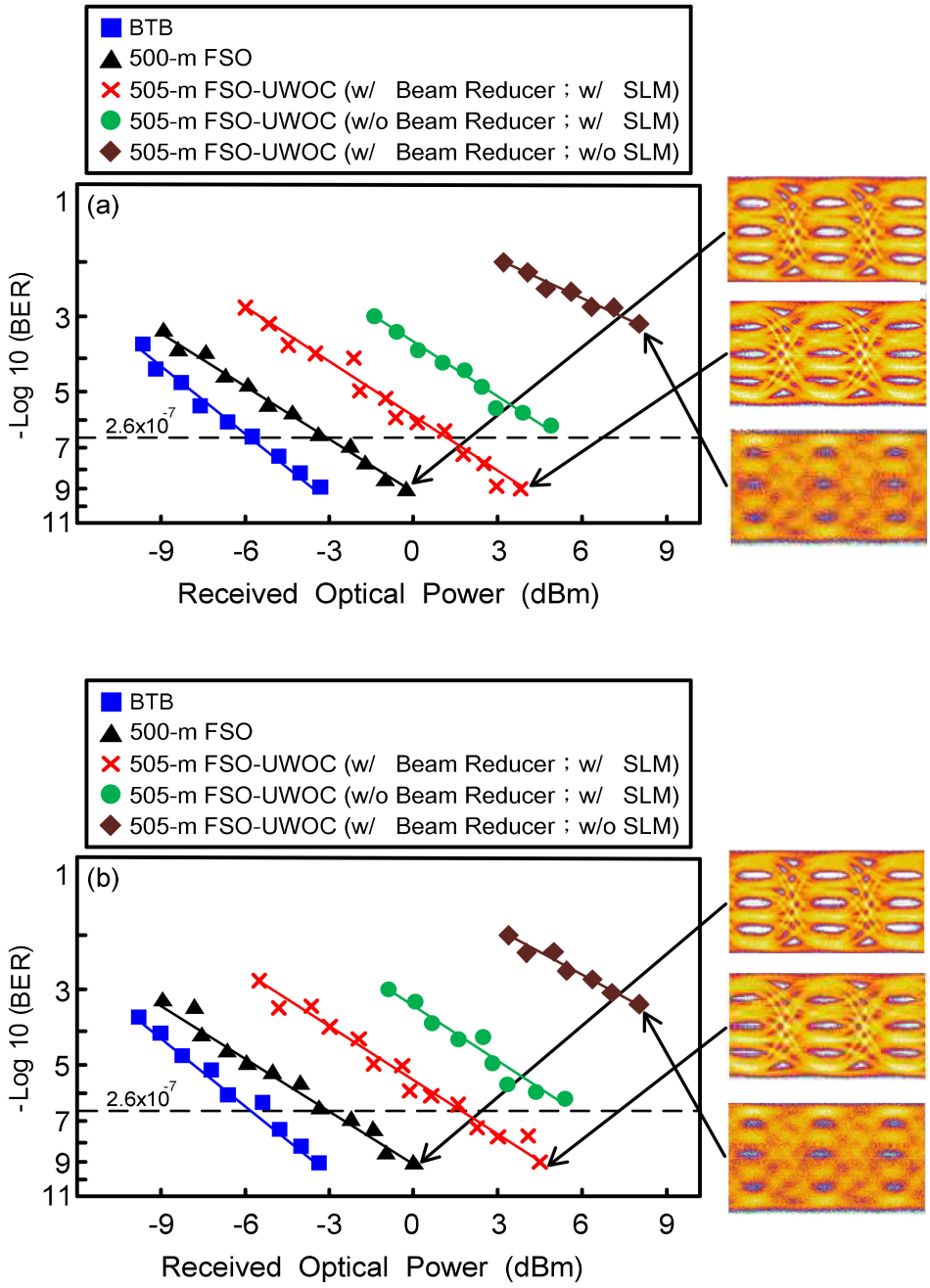

Fig. 8. (a) BER performances of the 50 Gb/s PAM4 signal at a chosen wavelength of 405.01 nm in the states of BTB, through 500 m free-space transmission (500-m FSO), and through 500 m free-space transmission and 5 m clear ocean underwater link (505-m FSO–UWOC). (b) BER values of the 50 Gb/s PAM4 signal at a chosen wavelength of 450 nm in the scenarios of BTB, through 500 m free-space transmission (500-m FSO), and through 500 m free-space transmission and 5 m clear ocean underwater link (505-m FSO–UWOC). BTB, back-to-back.

BER. The key concern is to adapt the beam size to the ferrule's active area to avoid large coupling loss. Since the laser beam is extremely narrow and the ferrule's active area is very small, the fiber's ferrule must be accurately placed at the back focal point of doublet lens 2 to obtain accepted laser beam alignment. Laser beam misalignment will lead to obvious BER performance degradation. Various performance mitigation techniques, such as multiple beam transmissions, increasing receiver FOV, adaptive optics, hybrid FSO/MMW, packet re-transmission, network rerouting, and OAM, can be adopted so as to have high link availability and reliability in FSO communications [46]. Regarding temperature turbulence, misalignment in the presence of temperature turbulence will defocus the laser and introduce signal fading. However, the temperature turbulence becomes strong enough to affect the free-space transmission when the temperature variation reaches 100 °C [25], [47]–[49], indicating that temperature turbulence has a very limited effect on FSO communications. In addition, with a 10^{-9} BER operation, a 4.3-dB [Fig. 8(a)]/4.5-dB [Fig. 8(b)] power penalty appears between the state through a 500-m free-space transmission and

that through a 500-m free-space transmission and 5-m clear ocean underwater link (with a laser beam reducer and SLM). The 4.3 dB/4.5 dB power penalty primarily results from the absorption owing to the 5 m clear ocean underwater link and coupling loss for laser beam coupling to the fiber's ferrule. A 5-m clear ocean underwater link produces absorption to some extent because absorption is a substantial contributor in the clear ocean underwater channel, and this condition worsens optical signal-to-noise ratio (OSNR) and BER.

To have more associations with the laser beam reducer, SLM, and BER performance, we remove the laser beam reducer and SLM separately to evaluate the BER performances over 500 m free-space transmission with 5 m clear ocean underwater link. With a laser beam reducer and an SLM, BER reaches 10^{-9}. Without a laser beam reducer but with an SLM, BER achieves a value of 8.6×10^{-7} [Fig. 8(a)]/9.2×10^{-7} [(Fig. 8(b)]. BER performance decreases with an increase in beam size. A smaller beam size that follows a lower absorption contributes more light being received by the PD with a TIA receiver, which results in better BER. In addition, the BER seriously declines to 4.7×10^{-4} [Fig. 8(a)]/4.6×10^{-4} [Fig. 8(b)] when in the state with a laser beam reducer but without an SLM. After a period of time, laser beam misalignment because of the flow of ocean becomes noticeably large. By way of a transmissive SLM with electrical controller, the laser beam can be adjusted to make up for the BER degradation on account of laser beam misalignment. With an SLM, the BER reaches a $10^{-7}/10^{-9}$ order of magnitude; without an SLM, the BER seriously declines to a 10^{-4} order of magnitude. A transmissive SLM with an electrical controller greatly improves the BER performance.

In addition, to verify the relation between the equalizer and the BER performance, we take away the equalizer at the receiving end and measure the BER values over 500 m free-space transmission with 5 m clear ocean underwater link at a filtered wavelength of 405.01 nm. With a laser beam reducer and an SLM, BER attains a value of 2.6×10^{-7} in the state without an equalizer. Whereas BER gets better to 10^{-9} in the state with an equalizer. The equalizer's function is to increase the levels of high frequencies, compared to the levels of low frequencies, and bring on an increased SNR and an enhanced BER. Accordingly, for this real-time WDM PAM4 FSO–UWOC integrated system without employing an equalizer at the receiving end, a BER value of $\leq 2.6 \times 10^{-7}$ satisfies the communication criterion.

In view of PAM4 eye diagrams, three independent clear eye diagrams are attained for the state through a 500-m FSO link. For the state through a 505-m FSO–UWOC link (with a laser beam reducer and an SLM), eye diagrams with qualified feature are obtained. For the state through a 505-m FSO–UWOC link (with a laser beam reducer but without an SLM), however, turbid eye diagrams are acquired.

IV. Conclusion

A laboratory setup of a dual-wavelength WDM PAM4 FSO–UWOC integrated system through a 500-m free-space transmission and 5-m clear ocean underwater link is established. Large 3-dB bandwidth enhancement and optical output power increment are attained using 405 nm blue-violet-light and 450 nm blue-light LDs with two-stage light injection and optoelectronic feedback techniques. Combining WDM scenario and PAM4 modulation, the channel capacity is greatly improved with a gross transmission rate of 100 Gb/s. With the adoption of doublet lenses in FSO communications, laser beam reducer and transmissive SLM in UWOC links, a sufficiently low BER of 10^{-9} and qualified PAM4 eye diagrams are attained through a 500-m free-space transmission and 5-m clear ocean underwater link. This demonstrated PAM4 FSO–UWOC integrated system meets the target of high-speed FSO–UWOC integration given its practicability for affording a high-transmission-rate over 500 m free-space transmission with 5 m clear ocean underwater link. It outperforms existing FSO–UWOC integrated systems and brings critically important developments characterized by optical wireless communications for affording high aggregate channel capacity with long-reach optical wireless transmission. For the future extension of this study, we aim to construct a high-speed WDM PAM4 FSO–UWOC integrated system in a real sea or ocean environment to resolve the practical engineering problems and enhance the scenario implemented by the integration of FSO and UWOC.

References

[1] L. Y. Wei, C. W. Hsu, C. W. Chow, and C. H. Yeh, "40-Gbit/s visible light communication using polarization-multiplexed R/G/B laser diodes with 2-m free-space transmission," in *Proc. Conf. Opt. Fiber Commun.*, Mar. 2019, Paper M3I.3.

[2] W. Y. Lin *et al.*, "10 m/500 Mbps WDM visible light communication systems," *Opt. Express*, vol. 20, no. 9, pp. 9919–9924, Apr. 2012.

[3] A. Al-Halafi and B. Shihada, "UHD video transmission over bidirectional underwater wireless optical communication," *IEEE Photon. J.*, vol. 10, no. 2, Apr. 2018, Art. no. 7902914.

[4] A. Al-Halafi, H. M. Oubei, B. S. Ooi, and B. Shihada, "Real-time video transmission over different underwater wireless optical channels using a directly modulated 520 nm laser diode," *IEEE/OSA J. Opt. Commun. Netw.*, vol. 9, no. 10, pp. 826–832, Oct. 2017.

[5] W. S. Tsai, C. Y. Li, H. H. Lu, Y. F. Lu, S. C. Tu, and Y. C. Huang, "256 Gb/s four-channel SDM-based PAM4 FSO-UWOC convergent system," *IEEE Photon. J.*, vol. 11, no. 2, Apr. 2019, Art. no. 7902008.

[6] M. S. Islam, M. Younis, and A. Ahmed, "Communication through air water interface using multiple light sources," in *Proc. IEEE Int. Conf. Commun.*, May 2018.

[7] M. V. Jamali, A. Chizari, and J. A. Salehi, "Performance analysis of multi-hop underwater wireless optical communication systems," *IEEE Photon. Technol. Lett.*, vol. 29, no. 5, pp. 462–465, Mar. 2017.

[8] J. Wang, C. Tian, X. Yang, W. Shi, Q. Niu, and T. A. Gulliver, "Underwater wireless optical communication system using a 16-QAM modulated 450-nm laser diode based on an FPGA," *Appl. Opt.*, vol. 58, no. 16, pp. 4553–4559, Jun. 2019.

[9] W. S. Tsai, H. H. Lu, H. W. Wu, C. W. Su, and Y. C. Huang, "A 30 Gb/s PAM4 underwater wireless laser transmission system with optical beam reducer/expander," *Sci. Rep.*, vol. 9, Jun. 2019, Art. no. 8605.

[10] P. Saboureau, J. P. Foing, and P. Schanne, "Injection-locked semiconductor lasers with delayed optoelectronic feedback," *IEEE J. Quantum Electron.*, vol. 33, no. 9, pp. 1582–1591, Sep. 1997.

[11] Y. Cao, Y. Zhao, J. Wang, X. Yu, Z. Ma, and J. Zhang, "Cost-efficient quantum key distribution (QKD) over WDM networks," *IEEE/OSA J. Opt. Commun. Netw.*, vol. 11, no. 6, pp. 285–298, May 2019.

[12] X. H. Huang *et al.*, "WDM free-space optical communication system of high-speed hybrid signals," *IEEE Photon. J.*, vol. 10, no. 6, Dec. 2018, Art. no. 7204207.

[13] T. Kodama *et al.*, "Demonstration of PAM4-OCDM system with electrical amplitude-level pre-tuning and post-equalization for data centers applications," *Opt. Express*, vol. 27, no. 8, pp. 11227–11235, Apr. 2019.

[14] Y. Pan, L. Yan, A. Yi, L. Jiang, W. Pan, and B. Luo, "Simultaneous demultiplexing of 2 × PDM-PAM4 signals using simplified receiver," *Opt. Express*, vol. 27, no. 3, pp. 1869–1876, Feb. 2019.
[15] G. W. Lu *et al.*, "Flexible generation of 28 Gbps PAM4 60 GHz/80 GHz radio over fiber signal by injection locking of direct multilevel modulated laser to spacing-tunable two-tone light," *Opt. Express*, vol. 26, no. 16, pp. 20603–20613, Aug. 2018.
[16] C. H. Yeh, W. P. Lin, C. M. Luo, Y. R. Xie, Y. J. Chang, and C. W. Chow, "Utilizing single lightwave for delivering baseband/FSO/MMW traffics simultaneously in PON architecture," *IEEE Access*, vol. 7, pp. 138927–138931, 2019.
[17] A. S. Fletcher, S. A. Hamilton, and J. D. Moores, "Undersea laser communication with narrow beams," *IEEE Commun. Mag.*, vol. 53, no. 11, pp. 49–55, Nov. 2015.
[18] C. Y. Li, H. H. Lu, X. H. Huang, Y. C. Wang, J. C. Chang, and P. H. Chew, "52 m/9 Gb/s PAM4 plastic optical fiber-underwater wireless laser transmission convergence with a laser beam reducer," *Chin. Opt. Lett.*, vol. 16, no. 5, May 2018, Art. no. 050101.
[19] B. M. Cochenour, L. J. Mullen, and A. E. Laux, "Characterization of the beam-spread function for underwater wireless optical communications links," *IEEE J. Ocean. Eng.*, vol. 33, no. 4, pp. 513–521, Oct. 2008.
[20] C. I. Zhang, H. Wei, Z. Liu, and X. Fu, "Characteristic ocean flow visualization using Helmholtz decomposition," in *Proc. Oceans — MTS/IEEE Kobe Techno-Oceans*, May 2018.
[21] Y. Shen *et al.*, "Flow velocity and temperature measuring in large scale wave-current flume by coastal acoustic tomography," in *Proc. Oceans MTS/IEEE Charleston*, May 2018.
[22] J. Carpenter, B. C. Thomsen, and T. D. Wilkinson, "Degenerate mode-group division multiplexing," *J. Lightw. Technol.*, vol. 30, no. 24, pp. 3946–3952, Dec. 2012.
[23] X. Sun, M. Kong, C. Shen, C. H. Kang, T. K. Ng, and B. S. Ooi, "On the realization of across wavy water-air-interface diffuse-line-of-sight communication based on an ultraviolet emitter," *Opt. Express*, vol. 27, no. 14, pp. 19635–19649, Jul. 2019.
[24] J. L. Wei, J. D. Ingham, D. G. Cunningham, R. V. Penty, and I. H. White, "Performance and power dissipation comparisons between 28 Gb/s NRZ, PAM, CAP and optical OFDM systems for data communication applications," *J. Lightw. Technol.*, vol. 30, no. 20, pp. 3273–3280, Oct. 2012.
[25] L. Zhang, H. Wang, X. Zhao, F. Lu, X. Zhao, and X. Shao, "Experimental demonstration of a two-path parallel scheme for m-QAM-OFDM transmission through a turbulent-air-water channel in optical wireless communications," *Opt. Express*, vol. 27, no. 5, pp. 6672–6688, Mar. 2019.
[26] Y. Zhao *et al.*, "Feedback-enabled adaptive underwater twisted light transmission link utilizing the reflection at the air-water interface," *Opt. Express*, vol. 26, no. 13, pp. 16102–16112, Jun. 2018.
[27] A. Wang *et al.*, "Adaptive water-air-water data information transfer using orbital angular momentum," *Opt. Express*, vol. 26, no. 7, pp. 8669–8678, Apr. 2018.
[28] Y. Chen *et al.*, "26 m/5.5 Gbps air-water optical wireless communication based on an OFDM-modulated 520-nm laser diode," *Opt. Express*, vol. 25, no. 13, pp. 14760–14765, Jun. 2017.
[29] A. Al-Halafi, "Real-time and ultra-high definition video transmission in underwater wireless optical networks," Ph.D. dissertation, Division Physical Sci. Eng., King Abdullah Univ. Sci. Technol., Thuwal, Saudi Arabia, 2018.
[30] M. Pittol, D. Tomacheski, D. N. Simões, V. F. Ribeiro, and R. M. C. Santana, "Evaluation of commercial $Mg(OH)_2$, $Al(OH)_3$ and TiO_2 as antimicrobial additives in thermoplastic elastomers," *Plastics, Rubber Composites*, vol. 46, no. 5, pp. 223–230, Apr. 2017.
[31] C. R. Coble, E. G. Murray, and D. R. Rice, *Earth Science*, 3rd ed. Englewood Cliffs, NJ, USA: Prentice-Hall, 1987, pp. 256–257.
[32] I. I. Kim, B. McArthur, and E. Korevaar, "Comparison of laser beam propagation at 785 nm and 1550 nm in fog and haze for optical wireless communications," *Proc. SPIE*, vol. 4214, pp. 26–37, Feb. 2001.
[33] H. Kaushal and G. Kaddoum, "Applications of lasers for tactical military operations," *IEEE Access*, vol. 5, pp. 20736–20753, 2017.
[34] J. Zhang *et al.*, "Fiber–wireless integrated mobile backhaul network based on a hybrid millimeter-wave and free-space-optics architecture with an adaptive diversity combining technique," *Opt. Lett.*, vol. 41, no. 9, pp. 1909–1912, May 2016.
[35] J. Wang, C. Lu, S. Li, and Z. Xu, "100 m/500 Mbps underwater optical wireless communication using an NRZ-OOK modulated 520 nm laser diode," *Opt. Express*, vol. 27, no. 9, pp. 12171–12181, Apr. 2019.
[36] X. Hong, C. Fei, G. Zhang, and S. He, "Probabilistically shaped 256-QAM-OFDM transmission in underwater wireless optical communication system," in *Proc. Opt. Fiber Commun. Conf.*, Mar. 2019, Paper Th2A.40.
[37] T. C. Wu, Y. C. Chi, H. Y. Wang, C. T. Tsai, and G. R. Lin, "Blue laser diode enables underwater communication at 12.4 Gbps," *Sci. Rep.*, vol. 7, Jan. 2017, Art. no. 40480.
[38] H. Kaushal and G. Kaddoum, "Underwater optical wireless communication," *IEEE Access*, vol. 4, pp. 1518–1547, 2016.
[39] Q. Peng, G. Chen, X. Li, Q. Liao, and Y. Guo, "Performance improvement of underwater continuous-variable quantum key distribution via photon subtraction," *MDPI Entropy*, vol. 21, no. 10, Oct. 2019. Art. no. 1011.
[40] M. V. Jamali, P. Nabavi, and J. A. Salehi, "MIMO underwater visible light communications: Comprehensive channel study, performance analysis, and multiple-symbol detection," *IEEE Trans. Veh. Technol.*, vol. 67, no. 9, pp. 8223–8237, Sep. 2018.
[41] L. J. Johnson, R. J. Green, and M. S. Leeson, "Underwater optical wireless communications: Depth-dependent beam refraction," *Appl. Opt.*, vol. 53, no. 31, pp. 7273–7277, Oct. 2014.
[42] J. Harriman, S. Serati, and J. Stockley, "Comparison of transmissive and reflective spatial light modulators for optical manipulation applications," *Proc. SPIE*, vol. 5930, Jul. 2005, Art. no. 59302D.
[43] I. E. Lee, Y. Guo, T. K. Ng, K. H. Park, M. S. Alouini, and B. S. Ooi, "Bandwidth enhancement of wireless optical communication link using a near-infrared laser over turbid underwater channel," in *Proc. Conf. Lasers Electro-Opt. Pacific Rim*, Nov. 2017, Paper 1921.
[44] C. Y. Li *et al.*, "A 5 m/25 Gbps underwater wireless optical communication system," *IEEE Photon. J.*, vol. 10, no. 3, Jun. 2018, Art. no. 7904809.
[45] J. Xu *et al.*, "Underwater wireless transmission of high-speed QAM-OFDM signals using a compact red-light laser," *Opt. Express*, vol. 24, no. 8, pp. 8097–8109, Apr. 2016.
[46] H. Kaushal and G. Kaddoum, "Optical communication in space: Challenges and mitigation techniques," *IEEE Commun. Surv. Tut.*, vol. 19, no. 1, pp. 57–96, Jan.–Mar. 2017.
[47] W. G. Alheadary *et al.*, "Free-space optical channel characterization and experimental validation in a coastal environment," *Opt. Express*, vol. 26, no. 6, pp. 6614–6628, Mar. 2018.
[48] S. A. Al-Gailani, A. B. Mohammad, M. S. Islam, U. U. Sheikh, and R. Q. Shaddad, "Tropical temperature and humidity modeling for free space optical link," *J. Opt.*, vol. 45, no. 1, pp. 87–91, Jan.–Mar. 2016.
[49] R. L. Phillips, *Laser Beam Propagation Through Random Media*, 2nd ed. Bellingham, WA, USA: SPIE Press, 2005.

Chung-Yi Li received the M.S. and Ph.D. degrees from the Department of Electro-Optical Engineering, National Taipei University of Technology (NTUT), Taipei, Taiwan, in 2008 and 2012, respectively. From 2013 to 2014, he was an Engineer with the Innovation and Product Development Department, FOCI Fiber Optic Communications, Inc., Hsinchu, Taiwan. In 2014, he joined the Department of Electro-Optical Engineering, NTUT, as a Research Assistant Professor. In 2018, he joined the Department of Communication Engineering, National Taipei University, New Taipei City, Taiwan, as an Assistant Professor. His research interests include FSO communications, UWOC systems, and FSO–UWOC integration.

Xu-Hong Huang received the M.S. degree from the College of Physics and Information Engineering, Fuzhou University, Fuzhou, China, in 2003. She joined the Fujian Hitachi TV as an Engineer in 1990 and was promoted to Senior Engineer in 2000. In 2003, she joined the School of Information Science and Engineering, Fujian University of Technology, Jin′an, Fuzhou, China as an Associate Professor. Her research interests include FSO communications, UWOC systems, and FSO–UWOC integration. She has authored or coauthored more than 25 papers in SCI-cited international journals and more than eight papers in international conferences.

Prof. Huang is currently a Fellow of the Fujian Electronics Society and a Fellow of the Fujian Electrical Engineering Society. She was the recipient of the Fujian Superior New Product Award in 1995, 1996, and 1998), the National Education Research Institute Excellent Paper Award (2009), and the Utility Model Invention Award (2013 and 2014).

Hai-Han Lu (SM'08) received the M.S. and Ph.D. degrees from the Institute of Optical Science, National Central University, Taoyuan City, Taiwan, in 1991 and 2000, respectively. In 2003, he joined the Department of Electro-Optical Engineering, National Taipei University of Technology, Taipei, Taiwan, as an Associate Professor. He was promoted to Professor, Distinguished Professor, and Lifetime Distinguished Professor in 2003, 2006, and 2017, respectively. His research interests include FSO communications, fiber-FSO convergence, UWOC systems, and FSO–UWOC integration. He has authored or coauthored more than 200 papers in SCI-cited international journals and more than 130 papers in international conferences.

Prof. Lu is currently a Fellow of SPIE, a Fellow of IET, and a Senior Member of OSA. He was the recipient of the Sun Yat-Sen Academic Award (Natural Science, 2017), National Invention Award (Gold Medal, 2016), ICT Month Innovative Elite Products Award (2014 and 2016), Outstanding Electrical Engineering Professor Award of the Chinese Institute of Engineering (2015), Outstanding Engineering Professor Award of the Chinese Engineer Association (2013), and Outstanding Research Award of NTUT (2004) for his significant technical contributions to FSO communications, fiber-FSO convergence, UWOC systems, and FSO–UWOC integration.

Yong-Cheng Huang was born in Changhua County, Taiwan, in December 1995. He received the B.S. degree from I-Shou University, Kaohsiung, Taiwan, in 2018. He is currently working toward the M.S. degree with the Institute of Electro-Optical Engineering, National Taipei University of Technology, Taipei, Taiwan. His research interests include FSO communications and UWOC systems.

Qi-Ping Huang was born in Nantou, Taiwan, in August 1996. He received the B.S. degree from Feng Chia University, Taichung, Taiwan, in 2018. He is currently working toward the M.S. degree with the Institute of Electro-Optical Engineering, National Taipei University of Technology, Taipei, Taiwan. His research interests include FSO communications and UWOC systems.

Shi-Cheng Tu was born in Taipei, Taiwan, in February 1995. He received the B.S. degree from the Ming Chi University of Technology, New Taipei City, Taiwan, in 2017. He is currently working toward the M.S. degree with the Institute of Electro-Optical Engineering, National Taipei University of Technology, Taipei, Taiwan. His research interests include FSO communications and UWOC systems.